KSME International Journal, Vol. 13, No. 9, pp. 585~595, 1999

Comparative Study of Tracking Control for a Mobile Manipulator: Nonholonomic and Dynamic Cases

Jae H. Chung* and Daehie Hong**

(Received March 9, 1998)

This paper gives an in-depth treatment of the modeling and control of a mobile manipulator which consists of a robotic manipulator mounted upon a mobile robot. By neglecting slip of the platform's tires, nonholonomic constraints are introduced into the equations of motion. By considering wheel slip, the assumption of nonholonomic motion is violated. Nonholonomic and dynamic models of a mobile manipulator are developed and compared using the Lagrange -d'Alembert formulation and the Newton-Euler method, respectively. The dynamic model which considers wheel slip incorporates a nonlinear tire friction model. The tracking problem is investigated by using input-output linearization for the nonholonomic model. For the dynamic model, a robust control method based on a matching condition is developed to eliminate the harmful effects of wheel slip, which acts as a disturbance to the system. Then, the effect of wheel slip on the tracking of commanded motion is identified via simulation. The effectiveness of the proposed control algorithm is demonstrated through computer simulation.

Key Words: Mobile Manipulator, Non-holonomic Constraint, Tracking Control

1. Introduction

Interest in the area of mobile manipulators has increased significantly in the industrial, military, and public service communities because of their mobility combined with manipulation. Their capabilities also allow them to perform complex tasks in environments inaccessible or very hazardous for humans. Although considerable research and development has been performed in the area of motion control of mobile manipulators, most of the models developed in the previous work assume only planar motion and/or holonomic constraints in which the complexity of the modeling and control problem is often excessively simplified.

Jang (1994) studied a single-linked manipulator on a planar wheeled platform and developed passive control systems to reduce the dynamic coupling between the two subsystems. Using a technique which is an extension of the energy stability level concept, Ghamsepoor and Sepehri (1995) developed a means to quantify stability measures applicable to mobile manipulators. Joshi and Desrochers (1986) represented the motion due to the mobile platform by an angular displacement (disturbance) to a two-linked arm. Their work took into account the effects of platform motion on the control of the robot arm relative to the platform. However, the control of the mobile platform was excluded. Hootsmanns and Dubowsky (1991) developed a mobile manipulator Jacobian transpose control algorithm which relies on vehicle motion sensing and the kinematic model of the system. Mobile manipulators with soft suspensions were shown to be stable with limited vehicle sensory data. However, only holonomic constraints were taken into account. Based upon the observation of a human-being's interaction with unknown environments, Chong

* Department of Mechanical and Aeronautical Engineering University of California, Davis, CA 95616 U.S.A.

** Department of Mechanical Engineering Korea University Seoul, Korea.

et al. (Chong et al., 1997) developed a joint-based control scheme to control the end-effector position of the manipulator which is tolerant to unexpected contact forces with the manipulator's environment. Liu and Lewis (1992) developed a robust controller for a mobile manipulator by considering the platform and the manipulator as two subsystems. However, they considered only translational motion of the mobile platform. Yamamoto and Yun (1994) studied a two-linked planar mobile manipulator subject to nonholonomic constraints and developed a coordination algorithm based on the concept of a preferred operating region. However, if the manipulator is commanded to follow a spatial trajectory in task space, the platform will not be able to position the manipulator at a specified point in the preferred region. Instead of the preferred operating region, Shibata et al. (Shibata et al., 1995) developed an equivalent mass matrix to determine robot motion performance and applied it to a planar mobile manipulator. Chung et al. (1998) considered a spatial mobile manipulator subject to kinematic redundancy. They developed an interaction control which consists of a robust adaptive controller for the manipulator and an input-output linearizing controller for the mobile platform. Using the configuration control scheme based on the kinematic model of a mobile manipulator, Seraji (1998) proposed an on-line approach in which mobility and manipulation are treated equally within a common framework.

Recently, Dugoff's pneumatic tire friction model is employed to describe the longitudinal and lateral forces acting on the wheels of the wheeled mobile robot for high load and high speed applications (Boyden and Velinsky, 1994). It is determined that the use of a kinematic model must be limited to lightweight vehicles which operate at very low speeds, low accelerations, and under lightly loaded conditions. This result motivates the dynamic modeling of the mobile manipulator subject to wheel slip.

The motivation for much of the previous work (Jang and Wiens, 1994; Ghamsepoor and Sepehri% 1995) stems from identifying the stability criteria so that the vehicle does not overturn. The work addressing mobile manipulators, e.g., off-line optimization methods (Pin et al., 1994), ignores the nonholonomic characteristic of the vehicle. Most of the models described in the previous work (Joshi and Desrochers, 1986; Liu and Lewis, 1990; Hootsmanns and Dubowsky, 1991; Yamamoto and Yun, 1994; Chung et al., 1998; Seraji, 1998) analyze the dynamic interaction in an explicit form. However, they have only planar motion and/or satisfy the assumption of nonholonomic motion which is far from realistic in practice.

In this paper, we first develop the nonholonomic equations of motion of a mobile manipulator using a Lagrange-d'Alembert formulation. In this formulation, the equations of motion are projected onto the subspace of allowable motions. This modeling scheme can also be directly applied to mobile manipulators subject to nonholonomic constraints with constrained manipulation. In the mobile robot literature, the majority of the mathematical models are based on pure kinematics of the platform. Even for dynamic models, a point mass is used to greatly simplify modeling effort and control design. In this paper, we deal with the full dynamic model of a nonredundant mobile manipulator with the driving wheels subject to nonholonomic constraints and wheel slip. The systematic modeling of mobile manipulators subject to nonholonomic constraints and the analysis of the dynamic model for control design are novel. Then, the solvability of tracking problems for the ideal model is investigated by using input-output feedback linearization. Furthermore, a robust control algorithm is developed for the dynamic model to minimize the harmful effect of wheel slip on tracking performance. Then, the effect of wheel slip on the tracking of commanded motion is identified in the simulation. The effectiveness of the proposed control algorithm is demonstrated through computer simulation.

2. Nonholonomic Modeling-Consideration of Ideal Velocity Constraints

The mobile manipulator shown in Fig. 1 is

considered. This mobile manipulator is supported by two independently driven wheels with a common platform-fixed axis and two passive, self-aligning wheels (casters). The detailed configuration of the mobile manipulator can be found in the freebody diagrams, Figs. 2 and 3, which are also used in deriving the dynamic equations of motion of the system subject to wheel slip. The wheeled platform is modeled as a nonholonomic system in which wheel slip is neglected due to slow motions. Hence, we assume that both lateral slip and longitudinal slip do not occur.

The equations of motion of a system subject to constraints can be written as

$$\frac{d}{dt}\frac{\partial L}{\partial \dot{\xi}}-\frac{\partial L}{\partial \xi}+\Psi^T(\xi)\lambda-\tau=0 \tag{1}$$

where $\Psi(\xi)\in R^{k\times n}$ represents a set of k velocity constraints, $\lambda=[\lambda_1, \cdots, \lambda_k]^T$ are Lagrange multipliers, $\xi=[\xi_1, \cdots, \xi_n]^T$ are a set of generalized coordinates for the system, L is the Lagrangian of the system, and τ corresponds to the generalized force vector.

In the absence of constraints, the robot's dynamic equations can be derived from the Euler-Lagrange equations. Given k such constraints, we can write them as a vector-valued set of k equations:

$$\Psi_j^i(\xi)\dot{\xi}=0,\ i=1, \cdots, k \text{ and } j=1, \cdots, n \tag{2}$$

Let the virtual displacement $\delta\xi$ be a vector which satisfies $\Psi(\xi)\delta\xi=0$. Then, $(\Psi^T(\xi)\lambda)\cdot\delta\xi=0$ for $\Psi(\xi)\delta\xi=0$ by D'Alembert's Principle. Since $(\Psi^T(\xi)\lambda)\cdot\delta\xi=0$, Eq. (1) becomes

$$\left(\frac{d}{dt}\frac{\partial L}{\partial \dot{\xi}}-\frac{\partial L}{\partial \xi}-\tau\right)\cdot\delta\xi=0 \tag{3}$$

The mobile platform is subject to one holonomic constraint and two nonholonomic constraints, written as

$$\phi=\frac{b}{d}(\xi_1-\xi_2), \tag{4}$$

$$\dot{y}_m\cos\phi-\dot{x}_m\sin\phi=0, \text{ and} \tag{5}$$

$$\dot{x}_m\cos\phi+\dot{y}_m\sin\phi=\frac{1}{2}r(\dot{\xi}_1+\dot{\xi}_2) \tag{6}$$

where ϕ is the heading angle of the platform, $[x_m\ y_m]$ is the position coordinate of the midpoint of the axle, ξ_1 is the angular displacement of the left wheel, and ξ_2 is the angular displacement of the right wheel.

We may write Eqs. (5) and (6) in matrix form with a vector ξ defined as

$$\xi=[\xi_1\ \xi_2\ \xi_3\ x_m\ y_m]^T \tag{7}$$

$\Psi(\xi)$, a set of velocity constraints, is given by

$$\Psi(\xi)=[\Psi_u(\xi)\ \Psi_c(\xi)] \tag{8}$$

where

$$\Psi_u(\xi)=\begin{bmatrix}0 & 0 & 0\\ \frac{1}{2}r & \frac{1}{2}r & 0\end{bmatrix} \text{ and} \tag{9}$$

$$\Psi_c(\xi)=\begin{bmatrix}-\sin\phi & \cos\phi\\ -\cos\phi & -\sin\phi\end{bmatrix} \tag{10}$$

Now, we derive the equations of motion using the Lagrange-d'Alembert formulation. Let $\delta\xi=[\delta\xi_1\ \delta\xi_2\ \delta\xi_3\ \delta x_m\ \delta y_m]^T$ represent a virtual displacement of the system. We obtain Eq. (3) with the set of velocity constraints as

$$\begin{bmatrix}0 & 0 & 0 & -\sin\phi & \cos\phi\\ \frac{1}{2}r & \frac{1}{2}r & 0 & -\cos\phi & -\sin\phi\end{bmatrix}\delta\xi=0 \tag{11}$$

Solving Eq. (11) for δx_m and δy_m gives

$$\delta x_m=\frac{1}{2}r(\delta\xi_1+\delta\xi_2)\cos\phi \text{ and} \tag{12}$$

$$\delta y_m=\frac{1}{2}r(\delta\xi_1+\delta\xi_2)\sin\phi \tag{13}$$

We redefine $\delta\xi$ as $\delta\xi_u=[\delta\xi_1\ \delta\xi_2\ \delta\xi_3]^T$ and $\delta\xi_c=[\delta x_m\ \ \delta y_m]^T$ where $\delta\xi_u$ is unconstrained and $\delta\xi_c$ is constrained. Using Eq. (8) and $\delta\xi=[\delta\xi_u\ \delta\xi_c]^T$, we obtain

$$\delta\xi_c=-\Psi_c^{-T}(\xi)\Psi_u(\xi)\delta\xi_u \tag{14}$$

It can be shown that the equations of motion become

$$\left(\frac{d}{dt}\frac{\partial L}{\partial \dot{\xi}_u}-\frac{\partial L}{\partial \xi_u}-\tau_u\right)-\Psi_u^T\Psi_c^{-T}\left(\frac{d}{dt}\frac{\partial L}{\partial \dot{\xi}_c}-\frac{\partial L}{\partial \xi_c}-\tau_c\right)=0 \tag{15}$$

Substituting the Lagrangian $L(\xi, \dot{\xi})$ into Eq. (15), the equations of motion of the mobile manipulator can be written as

$$D\ddot{\xi}_u+Q=\tau_u \tag{16}$$

where D and Q represent the inertia matrix and

the coupling force vector of the mobile manipulator, respectively.

3. Dynamic Modeling-Consideration of Wheel Slip

In the previous section, the equations of motion of the mobile manipulator were derived based on the assumption of nonholonomic motion which is never strictly achieved in practice, especially for high load and high speed applications. By considering slip of the wheeled platform's tires, the assumption of nonholonomic motion is violated. In this section, the dynamic equations of motion are derived using the Newton-Euler method and by incorporating Dugoff's nonlinear tire friction model which was developed experimentally. The free-body diagrams of the mobile manipulator are shown in Figures 2 and 3. For the dynamic equations of motion derived below, the body centered frames for the platform and the manipulator are used as can be seen in the free-body diagrams.

Given the angular velocities of the left and right wheels, ω_l and ω_r, the longitudinal and lateral velocities of the center of gravity, u and v, the yaw rate ω, and the longitudinal and lateral velocities of the left and right wheels, u_l and u_r can be written respectively as

$$u=\frac{1}{2}(u_l+u_r) \tag{17}$$

$$v=\frac{b}{d}(u_l-u_r)+v^s \tag{18}$$

$$\omega=\dot{\phi}=\frac{1}{d}(u_l-u_r) \tag{19}$$

$$u_l=r\omega_l-u_l^s, \text{ and} \tag{20}$$

$$u_r=r\omega_r-u_r^s \tag{21}$$

where ϕ is the angular displacement of the platform, v^s is the lateral slip speed of the wheel axle, u_l^s and u_r^s are the longitudinal slip speed of the centers of the left and right wheels, respectively, and r is the radius of the driving wheels. Furthermore, these equations have assumed that the platform is symmetric side-to-side such that the center of mass lies along its centerline. The acceleration of the center of mass of the manipulator can be obtained as $a_P=a_x\hat{i}+a_y\hat{j}+a_z\hat{k}$ where

$$a_x=\dot{u}-v\dot{\phi}-L_c\ddot{\theta}\sin\theta-L_c\dot{\theta}^2\cos\theta-L_c\dot{\phi}^2\cos\theta \tag{22}$$

$$a_y=\dot{v}+u\dot{\phi}+L_c\ddot{\phi}\cos\theta-2L_c\dot{\theta}\dot{\phi}\sin\theta, \text{ and} \tag{23}$$

$$a_z=-L_c\ddot{\theta}\cos\theta+L_c\dot{\theta}^2\sin\theta \tag{24}$$

Using Eqs. (22) ~ (24), the reaction forces and moment can be obtained as follows:

$$F_x=m_aL_c\ddot{\theta}\sin\theta+m_aL_c\dot{\theta}^2\cos\theta+m_aL_c\dot{\phi}^2\cos\theta-m_a\dot{u}+m_av\dot{\phi} \tag{25}$$

$$F_y=m_aL_c\dot{\theta}\dot{\phi}\sin\theta-m_aL_c\ddot{\phi}\cos\theta-m_a\dot{v}-m_au\dot{\phi}, \text{ and} \tag{26}$$

$$M_z=m_aL_c^2\dot{\theta}\dot{\phi}\sin\theta\cos\theta-(I_a+m_aL_c^2\cos^2\theta)\ddot{\phi}-m_aL_c\dot{v}\cos\theta+m_aL_cv\dot{\phi}\sin\theta \tag{27}$$

Now, the force and moment equations for the platform and the wheels can be written as

$$m_P(\dot{u}-v\dot{\phi})=F_{xrl}+F_{xrr}+F_x \tag{28}$$

$$m_P(\dot{v}+u\dot{\phi})=F_{yrl}+F_{yrr}+F_y \tag{29}$$

$$I_P\ddot{\phi}=M_z+\frac{d}{2}(F_{xrl}-F_{xrr})-b(F_{yrl}+F_{yrr}) \tag{30}$$

$$(I_a+maL_c^2)\ddot{\theta}-m_aL_c\dot{u}\sin\theta+m_aL_c^2\dot{\phi}^2\sin\theta\cos\theta+m_aL_av\dot{\phi}\sin\theta=\tau_a-m_agL_c\cos\theta \tag{31}$$

$$I_t\dot{\omega}_l=\tau_l-F_{xrl}r, \text{ and} \tag{32}$$

$$I_t\dot{\omega}_r=\tau_r-F_{xrr}r \tag{33}$$

where m_p is the mass of the platform, m_a is the mass of the arm, I_p is the moment of the inertia of the platform about a vertical axis, and I_a is the moment of inertia of the arm about the center of mass. The distance between the center of mass of the platform and the mid-point of the axle, b, is set to zero to obtain the dynamic equations of motion in a form that is more tractable for control design. Note that the dynamic equations of motion are not in closed form. The longitudinal and lateral forces on the wheels are calculated form Dugoff's tire friction model (Dugoff et al., 1970).

Substituting Eqs. (25)-(27) into Eqs. (28)-

(31) and rearranging the resulting equations, the dynamic equations of motion of the mobile manipulator can be written as

$$M\dot{\nu}+N+G=F \tag{34}$$

where $\dot{\nu}=[\dot{u}\ \ \dot{v}\ \ \ddot{\phi}\ \ \ddot{\theta}]^T$,

$$M=\begin{bmatrix} m_p+m_a & 0 & 0 & -m_aL_c\sin\theta \\ 0 & m_p+m_a & m_aL_c\cos\theta & 0 \\ 0 & m_aL_c\cos\theta & I_p+I_a+m_aL_c^2\cos^2\theta & 0 \\ -m_aL_c\sin\theta & 0 & 0 & I_a+m_aL_c^2 \end{bmatrix} \tag{35}$$

$$N=\begin{bmatrix} -m_aL_c\dot{\theta}^2\cos\theta-m_aL_c\dot{\phi}^2\cos\theta+m_pv\dot{\phi}-m_av\dot{\phi} \\ -m_aL_c\dot{\theta}\dot{\phi}\sin\theta+m_pu\dot{\phi}+m_au\dot{\phi} \\ -m_aL_c^2\dot{\theta}\dot{\phi}\sin\theta\cos\theta-m_aL_cv\dot{\phi}\sin\theta \\ m_aL_c^2\dot{\phi}^2\sin\theta\cos\theta+m_aL_cv\dot{\phi}\sin\theta \end{bmatrix} \tag{36}$$

$$G=\begin{bmatrix} 0 \\ 0 \\ 0 \\ m_aL_cg\cos\theta \end{bmatrix}, \text{ and} \tag{37}$$

$$F=\begin{bmatrix} F_{xrl}+F_{xrr} \\ F_{yrl}+F_{yrr} \\ \frac{1}{2}d(F_{xrl}-F_{yrl})-b(F_{yrl}+F_{yrr}) \\ \tau_a \end{bmatrix} \tag{38}$$

Now, the state variables are defined as $q_1=(x_e\ \ y_e\ \ z_e)^T$, $q_2=(u\ \ \dot{\phi}\ \ \dot{\theta})^T$, and $q=(q_1\ \ q_2)^T$. Eliminating the tire force terms and rearranging Eqs. (28)-(33), we obtain

$$\dot{q}=\mu+\xi\tau+\delta \tag{39}$$

where $\mu=(\mu_1\ \cdots\ \mu_6)$, $\xi=(0_{3\times3}\ \ T_{3\times3})^T$, $\delta=(\delta_x\ \ \delta_y\ \ \delta_z\ \ \delta_u\ \ \delta_\phi\ \ \delta_\theta)^T$, $\tau=(\tau_l\ \ \tau_r\ \ \tau_a)^T$,

$$\mu_1=u\cos\phi-L_c\dot{\theta}\sin\theta\cos\phi-L_c\dot{\phi}\cos\theta\sin\phi \tag{40}$$

$$\mu_2=u\sin\phi-L_c\dot{\theta}\sin\theta\cos\phi+L_c\dot{\phi}\cos\theta\sin\phi \tag{41}$$

$$\mu_3=0 \tag{42}$$

$$\mu_4=\frac{m_aL_c\dot{\theta}^2\cos\theta}{\Sigma_u}+\frac{m_aL_c\dot{\phi}^2\cos\theta}{\Sigma_u}-\frac{m_a^2L_c^3\dot{\phi}^2\sin^2\theta\cos\theta}{\Sigma_u\Sigma_a}-\frac{m_a^2L_c^2g\sin\theta\cos\theta}{\Sigma_u\Sigma_a} \tag{43}$$

$$\mu_5=\frac{m^aL_c^2\dot{\theta}\dot{\phi}\sin\theta\cos\theta}{\Sigma_\phi} \tag{44}$$

$$\mu_6=\frac{m_a^2L_c^2\dot{\theta}^2\sin^2\theta\cos\theta}{\Sigma_u\Sigma_a}+\frac{m_a^2L_c^2\dot{\phi}^2\sin\theta\cos\theta}{\Sigma_u\Sigma_a}-\frac{m_a^3L_c^4\dot{\phi}\sin^3\theta\cos\theta}{\Sigma_v\Sigma_a^2}-\frac{m_aL_c^2\dot{\phi}^2\sin\theta\cos\theta}{\Sigma_a}-\frac{m_a^3L_{cg}^3\sin^2\theta\cos\theta}{\Sigma_u\Sigma_a^2}-\frac{m_aL_{cg}\sin\theta\cos\theta}{\Sigma_a} \tag{45}$$

$$\xi=\begin{bmatrix} 0 & 0 & 0 \\ 0 & 0 & 0 \\ 0 & 0 & 0 \\ \frac{1}{r\Sigma_u} & \frac{1}{r\Sigma_u} & \frac{m_aL_c\sin\theta}{\Sigma_u\Sigma_a} \\ \frac{d}{2r\Sigma_\phi} & -\frac{d}{2r\Sigma_\phi} & 0 \\ \frac{m_aL_c\sin\theta}{r\Sigma_u\Sigma_a} & \frac{m_aL_c\sin\theta}{r\Sigma_u\Sigma_a} & \frac{m_a^2L_c^2\sin^2\theta}{\Sigma_u\Sigma_a^2}+\frac{1}{\Sigma_a} \end{bmatrix} \tag{46}$$

$$\delta=\begin{bmatrix} -v^s\sin\phi \\ v^s\cos\phi \\ 0 \\ (m_pr^2v^s\dot{\phi}-I_t(\dot{u}_l^s+\dot{u}_r^s))\frac{\Sigma_a}{\Sigma_u} \\ \frac{m_aL_c^2v_s\dot{\phi}\sin\theta}{\Sigma_\phi}-(\dot{u}_l^s-\dot{u}_r^s)\frac{dI_t}{\Sigma_\phi} \\ (m_pr^2v^s\dot{\phi}-I_t(\dot{u}_l^s+\dot{u}_r^s))\frac{m_aL_c\sin\theta}{\Sigma_u} \end{bmatrix} \tag{47}$$

$$\Sigma_a=I_a+m_aL_c \tag{48}$$

$$\Sigma_u=m_p+m_a+\frac{2I_t}{r^2}-\frac{m_a^2L_c^2\sin\theta}{\Sigma_a}, \text{ and} \tag{49}$$

$$\Sigma_\phi=I_p+I_a+m_aL_c^2\cos^2\theta+\frac{I_td^2}{2r^2} \tag{50}$$

4. Input-Output Linearization-The Nonholonomic Model

In this section, we derive the control law for the spatial mobile manipulator based on the model obtained using Eq. (15).

We first rewrite Eq. (16) as

$$\ddot{\xi}_u = H + D^{-1}\tau_u \tag{51}$$

where $H = -D^{-1}Q$.

Now, the state variables are defined as

$$\varphi = [\xi_u \;\; \dot{\xi}_u] \tag{52}$$

Eqs. (51) and (52) can be used to write

$$\dot{\varphi} = f(\varphi) + g(\varphi)\,\tau_u \tag{53}$$

Now we select the output associated with Eq. (53), $y = f(\xi_u)$, as the end-point of the manipulator. Differentiating each element of y twice allows terms involving elements of τ_u to appear. Then, the input-output description of the system Eq. (53) can be linearized using the following feedback:

$$\tau_u = F(\varphi) + G(\varphi)\,u \tag{54}$$

where

$$F(\varphi) = -DJ^{-1}\dot{J}\dot{\xi}_u - DH \text{ and} \tag{55}$$

$$G(\varphi) = -DJ^{-1} \tag{56}$$

Then, control system design of the mobile manipulator is then equivalent to a design problem of decoupled linear subsystems as follows:

$$\ddot{y} = \gamma \tag{57}$$

where gamma represents a new input to the system which is yet to be chosen.

5. Robust Control-The Dynamic Model

Now, we select the output associated with Eq. (39) as the end point of the mobile manipulator and define a new set of state variables as $x = (x_1\ x_2)^T$, $x_1 = [x_e\ y_e\ z_e]^T$, and $x_2 = [\dot{x}_e\ \dot{y}_e\ \dot{z}_e]^T$. Then, the transformation of the output equation into the global frame is performed. Differentiating the state vector x, we obtain the dynamic equation in the global frame as follows:

$$\dot{x} = \zeta(\phi,\ \theta,\ x,\ \delta) + \Phi(\phi,\ \theta,\ \delta)\,\tau + \eta(\phi,\ \theta,\ x,\ \delta) \tag{58}$$

where

$$\Phi(\phi,\ \theta,\ \delta) = \begin{bmatrix} 0_{3\times 3} \\ \Gamma(\phi,\ \theta,\ \delta) \end{bmatrix} \text{ and} \tag{59}$$

$$\Gamma(\phi,\theta,\delta) = \begin{bmatrix} \cos\phi & -L_a \sin\phi\cos\theta & -L_a\sin\theta\cos\phi \\ \sin\phi & L_a\cos\phi\sin\theta & L_a\sin\theta\sin\phi \\ 0 & 0 & L_a\cos\theta \end{bmatrix} \tag{60}$$

When wheel slip is neglected, the equations of motion are obtained as follows:

$$\dot{x}_N = \zeta_N(\phi,\theta,x) + \Phi_N(\phi,\theta)\,\tau \tag{61}$$

Define the following equations:

$$\Phi(\phi,\theta,\delta) = \Phi_N(\phi,\theta) + \Delta\Phi(\phi,\theta,\delta) \text{ and} \tag{62}$$

$$\zeta(\phi,\theta,x,\delta) = \zeta_N(\phi,\theta,x) + \Delta\zeta(\phi,\theta,x,\delta) \tag{63}$$

where $\Delta\zeta$ and $\Delta\Phi$ are the uncertainty terms. Then, $\Delta\Phi$ can be written as

$$\begin{aligned} \Delta\Phi(\phi,\theta,\delta) &= \begin{bmatrix} 0_{3\times 3} \\ \Delta\Gamma(\phi,\theta,\delta) \end{bmatrix} \\ &= \begin{bmatrix} 0_{3\times 3} \\ \Delta\Gamma_N(\phi,\theta) \end{bmatrix} \Delta\Gamma_N^{-1}(\phi,\theta)\,\Delta\Gamma(\phi,\theta,\delta) \\ &= \Phi_N(\phi,\theta)\,\Delta\Gamma_N^{-1}(\phi,\theta)\,\Delta\Gamma(\phi,\theta,\delta) \\ &= \Phi_N(\phi,\theta)\,\tilde{\Phi}(\phi,\theta,\delta) \end{aligned} \tag{64}$$

Similarly, it can be shown that

$$\Delta\zeta(\phi,\theta,x,\delta) = \Phi_N(\phi,\theta)\,\tilde{\zeta}(\phi,\theta,x,\delta) \text{ and} \tag{65}$$

$$\Delta\eta(\phi,\theta,x,\delta) = \Phi_N(\phi,\theta)\,\tilde{\eta}(\phi,\theta,x,\delta) \tag{66}$$

Then, ζ, Φ, and η can be rewritten respectively as

$$\zeta(\phi,\theta,x,\delta) = \zeta_N(\phi,\theta,x) + \Phi_N(\phi,\theta)\,\tilde{\zeta}(\phi,\theta,x,\delta) \tag{67}$$

$$\Phi(\phi,\theta,\delta) = \Phi_N(\phi,\theta) + \Phi_N(\phi,\theta)\,\tilde{\Phi}(\phi,\theta,\delta), \text{ and} \tag{68}$$

$$\eta(\phi,\theta,x,\delta) = \Phi_N(\phi,\theta)\,\tilde{\eta}(\phi,\theta,x,\delta) \tag{69}$$

Then, Eq. (58) is rearranged as

$$\dot{x} = \zeta_N(\phi,\theta,x) + \Phi_N(\phi,\theta)\,\tau + \rho(\phi,\theta,x,\delta) \tag{70}$$

where $\rho(\phi,\theta,x,\delta) = \Phi_N(\tilde{\zeta}(\phi,\theta,x,\delta) + \tilde{\Phi}(\phi,\theta,\delta) + \tilde{\eta}(\phi,\theta,x,\delta))$

Therefore, the dynamic equations of motion of the mobile manipulator in task space satisfy the

matching condition. It is well known that the matching condition is the structural form of a dynamic system to be satisfied for the application of a wide class of robust control algorithms.

Now, the position error and the velocity error are defined as

$$e_p = x_1 - x_1^d \text{ and} \tag{71}$$

$$e_d = x_2 - x_2^d \tag{72}$$

Then, the tracking error dynamics can be described as follows:

$$\dot{e} = Ae + B\{\chi + \eta - \dot{x}_2^d\} \tag{73}$$

where

$$e = (e_p \;\; e_d)^T \tag{74}$$

$$\chi = \dot{x}_2^d - K_d e_d - K_p e_p + \Delta\chi \tag{75}$$

$$\Delta\chi = \begin{cases} -\dfrac{\Phi_N^T P e}{\| \Phi_N^T P e \|}\bar{\rho}, & \text{for } \| \Phi_N^T P e \| \geq \epsilon \\ -\dfrac{\Phi_N^T P e}{\epsilon}\bar{\rho}, & \text{for } \| \Phi_N^T P e \| < \epsilon \end{cases} \tag{76}$$

K_p and K_d are the feedback gains, and the positive definite matrix P is the unique solution to the Lyapunov equation (Leitmann, 1981). The control design to follow is based on the premise that it may be possible to estimate worst case bounds on the effect of wheel slip on the tracking performance of the system. The control law χ is then designed to guarantee stability of Eq. (73). The norm bound of the uncertainty term ρ is obtained as

$$\| \rho \| = \| \Phi_N (\tilde{\zeta} + \tilde{\Phi} + \tilde{\eta}) \| \leq \bar{\rho} \tag{77}$$

The input-output description of Eq. (70) is linearized to cancel the nonlinearities using the following feedback:

$$\tau = \Phi_N^{-1}(\chi - \zeta_N) \tag{78}$$

Then, the combined system Eqs. (58) and (78) reduces to

$$\dot{x} = \chi + \rho \tag{79}$$

6. Simulation Results

In this section, computer simulation is conducted to examine the performance of the tracking controller designed for each model of the mobile manipulator developed throughout this paper. The parameters used in this simulation are $b=0$, $d=0.9144$m, $r=0.3048$m, $L_a=0.5$m, $L_c=0.25$m, $m_p=300$kg, $m_a=50$kg, $I_p=30$kg·m^2, and $I_a=10$kg·m^2, where b is the distance between the wheel baseline and the center of mass of the platform, d is the length of the wheel baseline, L_a is the length of the arm link, m_p is the mass of the platform, m_a is the mass of the arm, I_p is the moment of inertia of the platform, and I_a is the moment of inertia of the manipulator. The longitudinal and lateral tire coefficients, C_x and C_y, are set to 40034 N/rad and 40034 N/rad, respectively. Some of these parameters are chosen from Boyden et al. (1994), whose validity was proved through various experiments.

As mentioned in Sec. 3, Dugoff's tire friction model, which utilizes the frictional friction circle concept, is used as the basis for calculating tire forces. Basically, Dugoff's tire model is an empirical, nonlinear, discrete model which generates tire forces and, in turn, tire slip. As can be seen from Eqs. (67)-(69), $\tilde{\zeta}$, $\tilde{\Phi}$ and $\tilde{\eta}$ are those terms which include logitudinal and lateral slip speed. This can also be observed from Eqs. (17)-(21) which differentiate nonholonomic (or kinematic) model from dynamic models. Hence, due to the nonlinear and discrete nature of the tire model, it is not feasible to parametrize the slip velocities so that the norm bound of the uncertainty vector can be obtained analytically. In other words, the values of the parameters related to control design including $\bar{\rho}$ are to be determined judiciously basesd on repetitive attempts for improving tracking perfromance.

The following desired trajectory is used in the simulation:

Trajectory 1

$$x_d(t) = 3 + \sin t$$
$$y_d(t) = 3 + \cos t$$
$$z_d(t) = 0.6854 + 0.1 \sin t$$

In this simulation, the mobile manipulator is initially at rest, and the initial position of the end-effector is set to [3.3 4.3 0.7854], which is not on the desired trajectory. The control gains, K_p and K_d, are set to [6 6 12] and [3 3 8], respective-

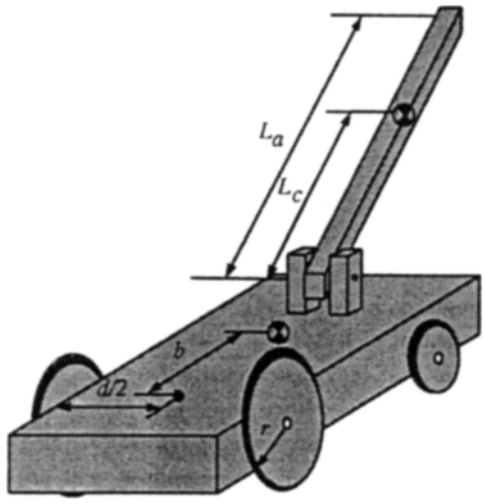

Fig. 1 The mobile manipulator.

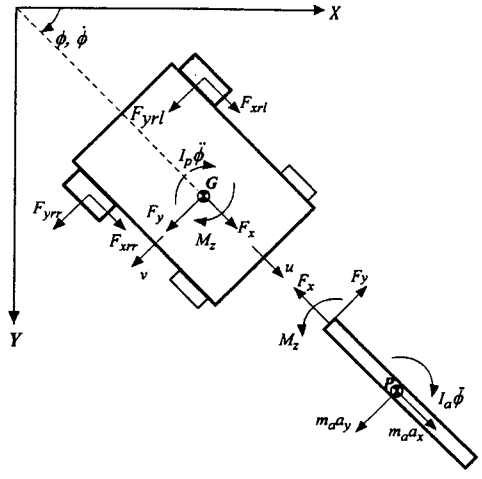

Fig. 2 Top view of the mobile manipulator.

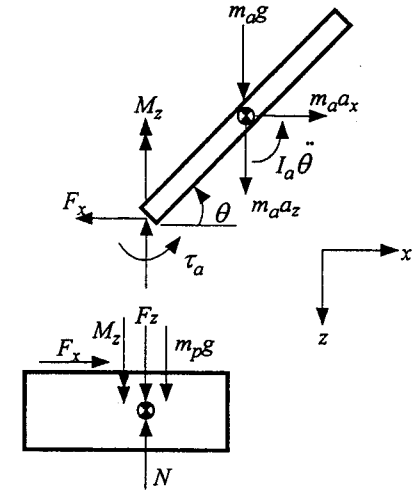

Fig. 3 Side view of the mobile manipulator.

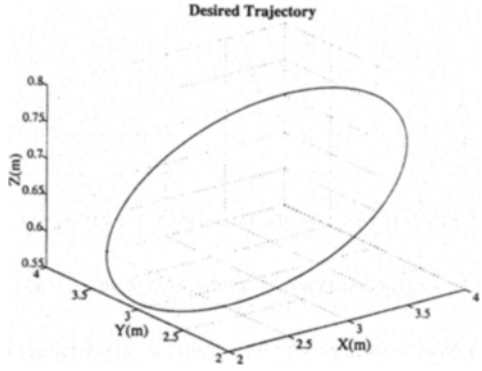

Fig. 4 Trajectory 1: the desired trajectory.

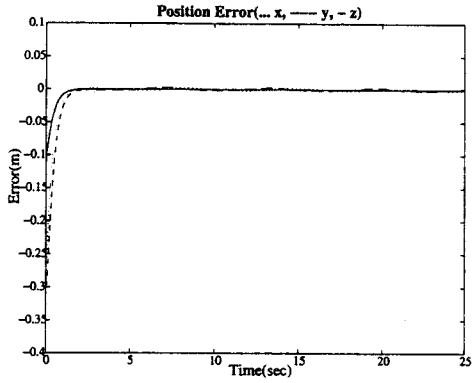

Fig. 5 Trajectory 1: position error-the nonholonomic model.

ly. The robust control parameters, ϵ and $\bar{\rho}$, are taken to be 0.01 and 2.75, respectively. In the simulation, the end-point of the mobile manipulator is commanded to follow the desired trajectory, and the platform is responsible for positioning the manipulator at a specified point in the workspace to avoid singular configurations of the system. The desired trajectory follows a circle in the x-y plane with a sinusoidal variation in the z direction. The mobile platform is ordered to adjust its heading in a sinusoidal manner to accommodate for the effects of the manipulator motion in the x-y plane due to the combination of the manipulator's vertical movements and the platform's yaw. Figure 4 shows the desired trajectory of the end-point of the manipulator in task

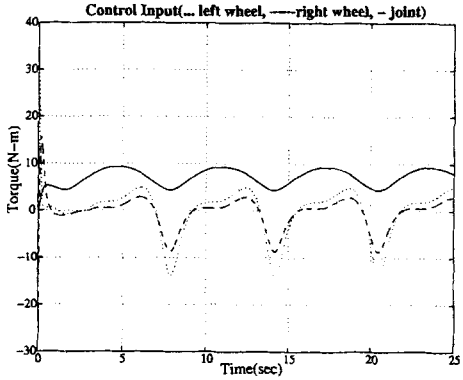

Fig. 6 Trajectory 1: control input-the nonholonomic model.

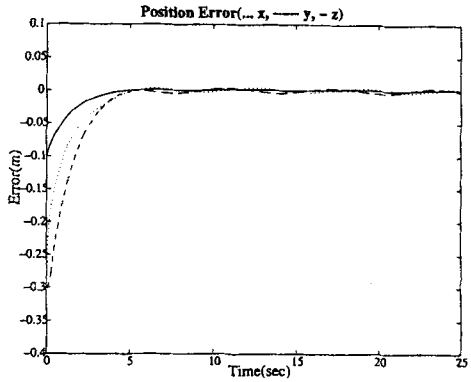

Fig. 9 Trajectory 1: position error with robust control-the dynamic model.

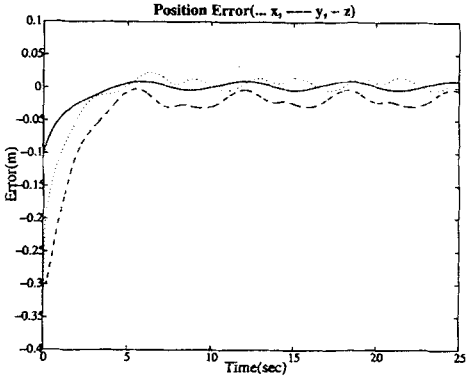

Fig. 7 Trajectory 1: position error without robust control-the dynamic model.

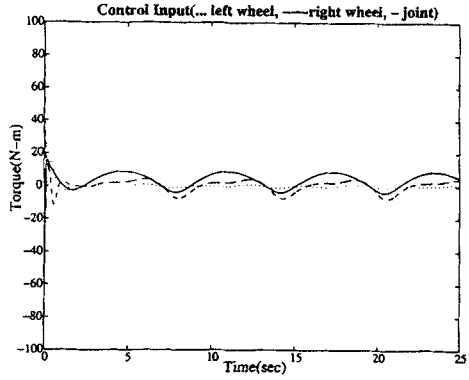

Fig. 10 Trajectory 1: control input with robust control-the dynamic model.

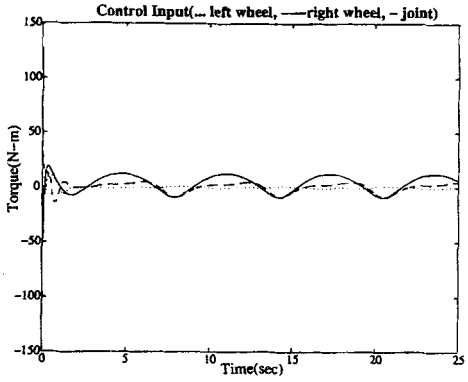

Fig. 8 Trajectory 1: control input without robust control-the dynamic model.

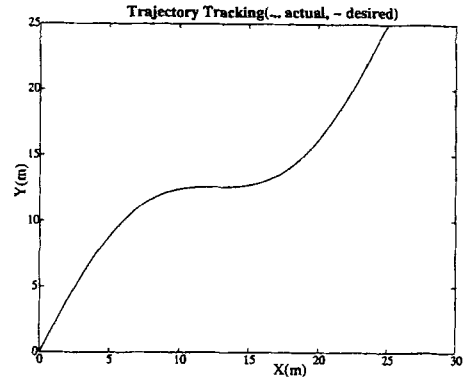

Fig. 11 Trajectory 2: tracking in the horizontal plane.

space. Figure 5 shows the tracking errors of the nonholonomic model-based controller in task space and demonstrates the excellent tracking performance as expected. Figure 7 depicts the best tuned tracking performance of the input-output linearizing controller for the mobile manipulator subject to wheel slip. It is obvious that the tracking performance degrades significantly in the

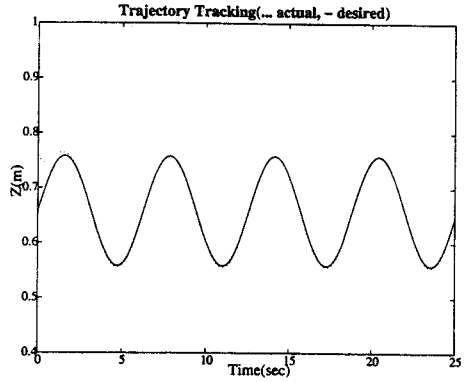

Fig. 12 Trajectory 2: tracking in the vertical plane.

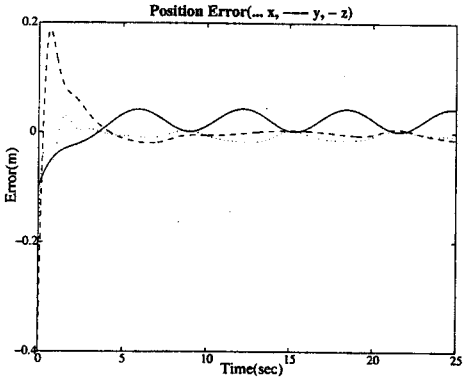

Fig. 13 Trajectory 2: position error without robust control.

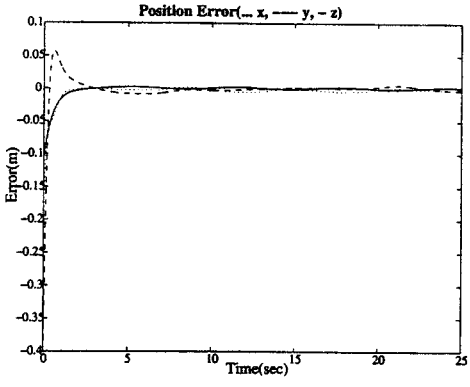

Fig. 14 Trajectory 2: position error with robust control.

presence of wheel slip. Figure 9 shows the tracking performance of the robust controller designed for the dynamic model of the mobile manipulator. It is observed that the tracking errors quickly converge to very small values compared to the non-robust control design. The control inputs for the control schemes are shown in Figs. 6, 8, and 10.

An additional reference trajectory was applied to further illustrate simulation results as follows:

Trajectory 2

$$x_d(t) = t$$
$$y_d(t) = t + 4\sin(t/4)$$
$$z_d(t) = 0.6854 + 0.1\sin t$$

Trajectory 2 follows a sinusoidal path in the x-y plane with a sinusoidal variation in the z direction similar to trajectory 1. It is noted that trajectory 2 represents a relatively fast motion of the platform which generates significant amount of tire forces and subsequently wheel slip. The same values of the control paremeters used for trajectory 1 were employed for this trajectory. The mobile manipulator is initially at rest, and the initial position of the end-effector is set to [0.2 0.3 0.7854]. Figures 11 and 12 show the desired and actual trajectories for the horizontal and vertical planes, respectively. It is observed that the desired and actual trajectories are almost identical after a few seconds of transient motion. Also, it is obvious from Figs. 13 and 14 that the additional feedback suppresses the tracking error to a small bounded value.

7. Conclusion

In this paper, we have developed the nonholonomic equations of motion of a mobile manipulator using the Lagrange-d'Alembert formulation. In this formulation, the equations of motion are projected onto the subspace of allowable motions. Then, the dynamic model of the mobile manipulator was developed for high load and high speed applications, in which Dugoff's tire friction model was incorporated. For the nonholonomic model, an input-output linearization method was utilized to solve the tracking problem. However, for high load and high speed conditions, inadequacy of applying the input-output linearizing controller was identified through simulation. Then, a robust controller was

designed to eliminate the harmful effects of the wheel slip on tracking performance. The effectiveness of the model-based robust controller is shown through computer simulation.

References

(1) Boyden, F. D. and Velinsky, S. A. (1994). Dynamic modeling of wheeled mobile robots for high load applications. In *Proceedings of IEEE International Conference on Robotics and Automation*, pp. 3071~3078.

(2) Chong, N. Y., Yokoi, K., Oh, S. R., and Tanie, K. (1997). Posiiton Control of collision-tolerant passive mobile manipulator with base suspension characteristics. In *Proceedings of IEEE International Conference on Robotics and Automation*, pp. 595~599.

(3) Chung, J. H., Velinsky, S. A., and Hess, R. A. (1998). Interaction control of a redundant mobile manipulator. *International Journal of Robotics Research*, Vol. 17, No. 12, pp. 1302~1309.

(4) Dugoff, H., Fancher, P., and Segal, L. (1970). An analysis of tire traction properties and their influence on vehicle dynamic performance. *SAE Transactions*, pp. 1219~1243.

(5) Ghamsepoor, A. and Sepehri, N. (1995). A measure of machine stability for moving base manipulators. In *Proceedings of IEEE International Conference on Robotics and Automation*, pp. 2249~2254.

(6) Hootsmanns, N. A. M. and Dubowsky, S. (1991). The motion control of manipulators on mobile vehicles. In *Proceedings of IEEE International Conference on Robotics and Automation*, pp. 2336~2341.

(7) Jang, W. M. and Wiens, G. J. (1994). Passive joint control of dynamic coupling in mobile robots. *International Journal of Robotics Research*, 3:209-220.

(8) Joshi, J. and Desrochers, A. A. (1986). Modeling and control of a mobile robot subject to disturbances. In *Proceedings of IEEE International Conference on Robotics and Automation*, pp. 1508~1513.

(9) Leitmann, G. (1981). On the efficacy of nonlinear control in uncertain linear systems. *Transactons of the ASME Journal of Dynamic Systems, Measurement, and Control*, 102:95-102.

(10) Liu, K. and Lewis, F. L. (1990). Decentralized continuous robust controller for mobile robots. In *Proceedings of IEEE International Conference on Robotics and Automation*, pp. 1822~1827.

(11) Pin, F. G., Culioli, J. C., and Reister, D. B. (1994). Using minimax approaches to plan optimal task commutation configurations for combined mobile paltform-manipualtor systems. *IEEE Transactions on Robotics and Automation*, 10(1):44~54.

(12) Seraji, H. (1998). A unified appraoach to motion control of mobile manipulators. *International Journal of Robotics Research*, 17(2): 107~118.

(13) Shibata, K., Murakami, T., and Ohnishi, K. (1995). Control of a mobile manipulator based on equivalent mass matrix. In *Proceedings of IEEE International Conference on Robotics and Automation*, pp. 1330~1335.

(14) Yamamote, Y. and Yun, X. (1994). Modeling and compensation of the dynamic interaction of a mobile manipulator. In *Proceedings of IEEE International Conference on Robotics and Automation*, pp. 2184~2192.